DISCRETE AND CONTINUOUS
DYNAMICAL SYSTEMS SERIES B
Volume **26**, Number **11**, November **2021**

doi:10.3934/dcdsb.2021232

pp. **5849–5871**

TRANSITIONS BETWEEN METASTABLE LONG-RUN CONSUMPTION BEHAVIORS IN A STOCHASTIC PEER-DRIVEN CONSUMER NETWORK

Jochen Jungeilges*

University of Agder, School of Business and Law
Department of Economics and Finance, Servicebox 422
N-4604 Kristiansand S, Norway
Ural Federal University, Institute of Natural Science and Mathematics
51 Lenin Avenue, Ekaterinburg 620000, Russian Federation

Trygve Kastberg Nilssen

University of Agder, School of Business and Law
Department of Economics and Finance, Servicebox 422
N-4604 Kristiansand S, Norway

Tatyana Perevalova

Ural Federal University, Institute of Natural Science and Mathematics
Ural Mathematical Center, 51 Lenin Avenue, Ekaterinburg 620000, Russian Federation

Alexander Satov

Ural Federal University, Institute of Natural Science and Mathematics
51 Lenin Avenue, Ekaterinburg 620000, Russian Federation

Abstract. We study behavioral change - as a transition between coexisting attractors - in the context of a stochastic, non-linear consumption model with interdependent agents. Relying on the indirect approach to the analysis of a stochastic dynamic system, and employing a mix of analytical, numerical and graphical techniques, we identify conditions under which such transitions are likely to occur. The stochastic analysis depends crucially on the stochastic sensitivity function technique as it can be applied to the stochastic analoga of closed invariant curves [14], [1]. We find that in a moderate noise environment increased peer influence actually reduces the complexity of observable long-run consumer behavior.

1. **Introduction.** We analyze the dynamics of a stochastic discrete-time system whose deterministic skeleton consists of a 2D noninvertible map which has an economic interpretation. Our study considers an economically meaningful subset of the parameter space associated with the *coexistence of attractors*. Each of these attractors can be thought of as the state-space representation of alternative long-run consumption behavior. In particular, we study the transition dynamics between the coexisting attractors and demonstrate that - irrespective of the type of stochastic perturbations considered - a study of the dynamic behavior can be facilitated two

2020 *Mathematics Subject Classification.* Primary: 37G35, 37H20; Secondary: 37N40.
Key words and phrases. Non-invertible maps, metastable attractors, escapes, transition.
The authors want to thank two anonymous referees for there work.
* Corresponding author: Jochen Jungeilges.

derivates of sensitivity analysis: confidence sets of attractors and the related critical noise intensities.

The paper tries to achieve two goals. First, we aim at extending previous work, by providing another example for the versatility of the stochastic sensitivity function technique (SSF) in the context of noise induced transition. Second, we devise a framework aimed at providing guidance for the analysis of noise induced transition in the presence of coexistence of attractors. We have not encountered a comparable formalization in the literature. The usefulness of the framework is demonstrate, by applying it to a dynamic stochastic consumption model.

To realize our objectives, we draw on developments and results from the study of (i) deterministic 2D-noninvertible maps, (ii) noise-induced transitions, and form the (iii) sensitivity analysis of dynamic systems.

Motivated by early work on endogenous preference change due to [3], [8] and [9] derived and analyzed a deterministic, non-linear model of the consumption process emphasizing non-market aspects of consumption. A rigorous re-analysis of the model has recently been provided by [5], [6]. Stochastic variants, with and without interaction between individuals, have been considered by [12], [11].

Sensitivity analyses reveal the effects of random perturbations on attractors of dynamic systems. Research in this area tends to rely on a *semi-analytical approach* due to [14]. The technique relies on the indirect method of studying stochastic dynamic systems. Recent examples for successful implementations of the technique include [20] who discuss noise induced extinction in a model of bacterial infection and [18] who study the effect of noise on attractors in a dynamic model of the cardiac action potential. [16] study noise-induced transitions in the context of coupled chaotic oscillators. Moreover, the stochastic sensitivity function methodology has been used to study the sensitivity of attractors in economic and financial models formulated in discrete time in [11] and [10].

Our stochastic consumption model is presented in Section 2. While Section 3 provides a review of some global structures of the *deterministic* nonlinear system in the area of multi-stability, Section 4 focuses on the *stochastic* dynamics prevailing in this region of coexisting attractors. Next, in Section 5, we introduce the stochastic sensitivity function (SSF) approach, outline its derivates central to our approach, and discuss how it can be integrated with concepts from deterministic dynamics to study transitions between coexisting attractors in a stochastic setting. Next, we use the resulting framework to study transition events between consumption behaviors in Sections 6 and 7. Relying on the concept of *critical noise intensities* in the former section, we adopt a space state perspective to *dissect* a transition event involving two types of closed invariant curves for the case of *additive* noise. Finally, we discuss our results and gather main conclusions in Section 8.

2. **The model.**

The background for our investigation of transitions between long-run consumption behaviors is constituted by work in dynamic microeconomics merging the concepts of endogenous preference adjustment and interdependencies between consumers. The model captures the economic as well as the social dimension of consumption in noisy environments.

Following [8] and [9], we consider two myopic utility-maximizing individuals, indexed by $i = 1, 2$, who consume amounts of two non-storable commodities x and y. At every time period, each individual equipped with an idiosyncratic preference order (assumed to be representable by a utility function) is endowed with a fixed

exogenous income b_i. Confronted with the time-invariant price system $p = (p_x, p_y)$, each individual chooses to consume $(x_{i\,t}, y_{i\,t})$ units of the respective commodities. This choice is optimal given the preferences held by the individual at time t. Running counter to mainstream microeconomics, we allow the individual's preference to vary between time periods in response to its own past consumption experience as well as the past consumption of the respective other individual. Moreover, we consider both *additive* and *parametric noise*. While the former models additive shocks to quantities purchased, the latter considers an informational asymmetry in the sense that one individual is uncertain about the income of the other individual while the other individual is fully informed.

Since we assume that an individual's consumption expenditure for units of the commodities x and y exhausts its income, the consumption dynamics can be described in terms of commodity x only. The demand for commodity x in time evolves according to the non-linear stochastic difference equation

$$x_{t+1} = f(x_t) + \varepsilon g(x_t)\xi_t, \tag{1}$$

where f represents the 2D noninvertible map $f : \mathbb{R}^2_+ \to \mathbb{R}^2_+$

$$f(x_t) = \begin{pmatrix} \frac{b_1}{p_x p_y}\left(\alpha_1 x_{1t}(b_1 - p_x x_{1t}) + D_{12} x_{2t}(b_2 - p_x x_{2t})\right) \\ \\ \frac{b_2}{p_x p_y}\left(\alpha_2 x_{2t}(b_2 - p_x x_{2t}) + D_{21} x_{1t}(b_1 - p_x x_{1t})\right) \end{pmatrix} \tag{2}$$

and g denotes the smooth matrix function

$$g(x_t) = \begin{pmatrix} \iota_1 \frac{b_1 D_{12}}{p_x p_y} x_{2t} & \iota_2 & 0 \\ \\ 0 & 0 & \iota_3 \end{pmatrix}. \tag{3}$$

The real, strictly positive, parameters α_1, α_2 and D_{12}, D_{21} are referred to as *learning* and *influence* parameters respectively. The shocks $\xi_t = (\xi_{0t}, \xi_{1t}, \xi_{2t})^\top$ are assumed to follow a *tri*-variate Gaussian white-noise process with $\mathbb{E}[\xi_t] = 0$ and $\mathbb{V}[\xi_t] = I_{(3,3)}$ for all t, where I denotes the identity matrix. The scalar constant $\varepsilon \geq 0$ takes the role of a noise intensity. In the sequel, we will focus on two specifications of the binary vector $\iota_{(1,3)} = (\iota_1, \iota_2, \iota_3)$: while $\iota_{(1,3)} = (0, 1, 1)$ is consistent with additive noise, $\iota_{(1,3)} = (1, 0, 0)$ refers to the case of parametric noise.

The feasible region for the deterministic skeleton ($\varepsilon = 0$) is given in the following definition.

Definition 2.1. If $\alpha_1 b_1^2 + D_{12} b_2^2 < 4 p_x p_y, \quad \alpha_2 b_2^2 + D_{21} b_1^2 < 4 p_x p_y$ holds, then $f(S) \subset S$ where

$$S = \left(0, \frac{b_1}{p_x}\right) \times \left(0, \frac{b_2}{p_x}\right) \tag{4}$$

is the feasible phase region.

As detailed in [11] it is possible to identify sets of parameter values implying economically meaningful trajectories with high probability. All experiments discussed in later sections were designed such that the consumption trajectories are economically meaningful. Throughout the paper, we consider a *fixed economic environment* of prices and incomes: $p = (p_x, p_y) = \left(\frac{1}{4}, 1\right)$, $b = (b_1, b_2) = (10, 20)$. Beyond that, we assume that the adjustment of individual preferences is mainly driven by the past consumption of an individual's peer. The effect of the own past consumption is weak. Thus fixing the learning parameters at low values $\alpha_1 = 0.0002$, $\alpha_2 = 0.00052$

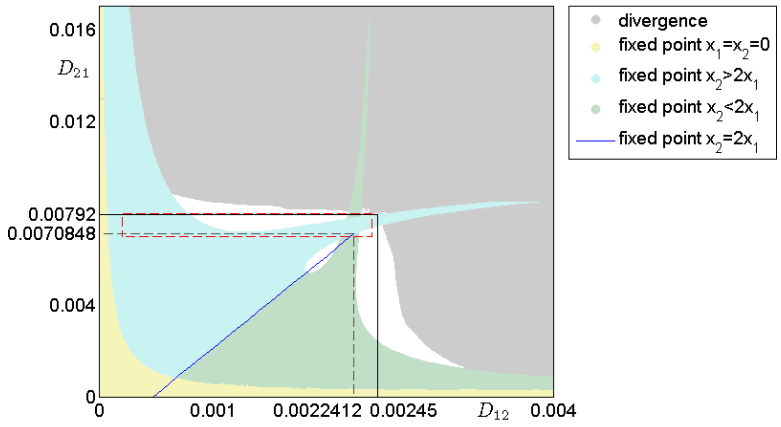

FIGURE 1. Bird's eye view of the parameter plane D, where remaining parameters have been fixed at $(p_x, p_y) = \left(\frac{1}{4}, 1\right)$, $(b_1, b_2) = (10, 20)$, $\alpha_1 = 0.0002$, $\alpha_2 = 0.00052$.

and using Definition 2.1, we derive a set of admissible values for the influence parameters as

$$D^e = \{(D_{12}, D_{21}) \mid 0 \leq D_{12} \leq 0.00245 \wedge 0 \leq D_{21} \leq 0.00792\}. \tag{5}$$

The dynamic phenomena discussed below are associated with a subset of D^e.

Given its preferences and the economic environment (b_i, p) at time t, individual i has no incentive to deviate from the choice $(x_{i\,t}, y_{i\,t})$ during period t. Any trajectory $\{x_t\}_{t=1}^T$ thus can be viewed as a sequence of T consecutive household equilibria for the two myopic individuals considered. The units purchased of commodity y are implicit. This interpretation holds in the deterministic as well as in the stochastic cases. A trajectory therefore reflects dynamic consumption behavior of myopic individuals. A trajectory that has settled on or stays close to an attractor of the system (1) is indicative of long-run consumption behavior. If a trajectory leaves an attractor to settle down on another one, then we refer to the associated consumption behavior as transitory.

3. **Dynamic modes of the deterministic skeleton.** In Figure 1, we present a 2D-bifurcation diagram for the subset $D = \{(D_{12}, D_{21}) \mid 0 \leq D_{12} \leq 0.004 \wedge 0 \leq D_{21} \leq 0.016\}$ of the parameter plane (D_{12}, D_{21}). The set $D^N = \{(D_{12}, D_{21}) \mid 0.0002 \leq D_{12} \leq 0.0024 \wedge 0.007 \leq D_{21} \leq 0.008\}$, i.e. the rectangle formed by red broken lines, represents the area of interest in the study at hand. $D^N \subset D^e$ is situated close to the Northern boundary of the set D^e associated with economically meaningful consumption trajectories. The region below this rectangle has been studied extensively in [11]. The authors identify coexisting fixed points and 2-cycles of the deterministic skeleton and analyze the transition phenomena occurring in the context of the associated stochastic model. In our current effort, we focus on the said rectangular region since coexisting complex attractors are found for these parameter values in the deterministic case. In the presence of additive and/or parametric noise these subsets of the parameter plane are predestined to give rise to intricate transition phenomena. Seen from the economic perspective, we are

focussing on a region of the parameter space in which noise-induced transitions might occur between alternative types of long-run consumption behavior.

In particular, the rectangle marked by red broken lines is partitioned into parameter constellations (D_{12}, D_{21}) colored light blue, light green, and white. Light blue (green) indicates that the deterministic map (1)($\varepsilon = 0$) possesses a fixed point such that the long-run consumption of the high-income individual 2 is at least (at most) twice as high as the consumption of individual 1. So far, the white region constitutes *terra incognita* an area of unknown and uncharted complex long-run dynamics.

3.1. **Characterizing D^N by 2D-bifurcation diagrams.** A first glimpse at the various dynamic modes existing over the subset D^N is provided by Figure 2. The graph in Figure 2 shows a selection of dynamical modes that can be observed in the (D_{12}, D_{21}) plane along with the prominent Neimark–Sacker bifurcation curve NS. This curve is constituted by those geometric *loci* at which the stable fixed point becomes an unstable focus and a closed invariant curve (Γ) emerges. While inside the white partition, *quasi-periodic* attractors and high-period attracting cycles dominate, the said area is interspersed with periodicity regions of attracting cycles of low periods. Points (D_{12}, D_{21}) lying in an intersection of periodicity regions are associated with the *coexistence of attractors.*

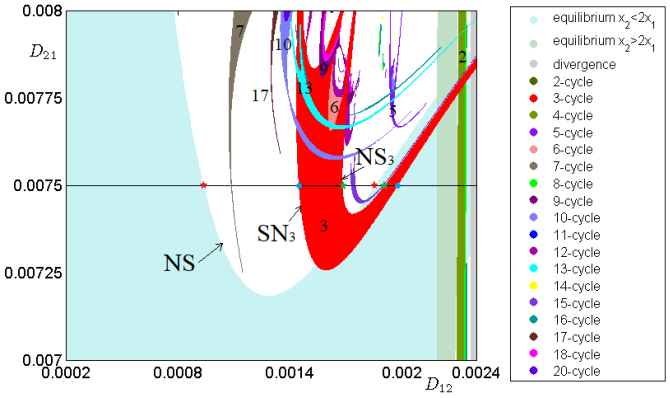

FIGURE 2. Bifurcation diagram for D^N with $(p_x, p_y) = \left(\frac{1}{4}, 1\right)$, $(b_1, b_2) = (10, 20)$, $\alpha_1 = 0.0002$, $\alpha_2 = 0.00052$. NS indicates the Neimark-Sacker bifurcation curve related to the fixed point. SN_3 curve gives the *loci* at which a saddle 3-cycle is born together with the attracting 3-cycle (C_3) via a saddle-node bifurcation. NS_3 designates the Neimark-Sacker bifurcation curve of the 3-cycle. The horizontal line through $D_{21} = 0.0075$ indicates the interval of parameter values for which our study of transitions between coexisting attractors focuses on. The NS and NS_3 curves are crossed twice at $\star$ (red star) and $\star$ (green star). Also the saddle node bifurcation curve SN_3 is intersected twice. The intersection points are indicated by $\bullet$ (blue circles). Related details are revealed in Figure 3.

Some of the periodicity regions Π_k show the characteristics of resonance tongues (Arnold or mode-locking tongues).

Definition 3.1. Let Π_k denote a connected set of parameter values issued from a Neimark-Sacker bifurcation curve such that for every $p = (D_{12}, D_{21})$ and $p \in \Pi_k$, there exists a stable period k-cycle. Π_k is called a period k-resonance tongue.

In Figure 2, a resonance tongue Π_7 is clearly visible. [1] For parameter values sufficiently close to the bifurcation curve NS, the boundary of a tongue is constituted by those points in parameter space at which the k-periodic points disappear in the course of a saddle-node bifurcation. The nature of the boundary might change at parameter values distant from the Neimark-Sacker curve. There *may*, for instance, exist the boundary related to a flip bifurcation of the stable k-cycle. Consequently, the k-cycle may exist outside Π_k.

Only periodicity regions up to order $k \leq 20$ are indicated in Figure 2. Many of the regions have the characteristic shape of a *sickle* or a *reaping hook*. Most of them do not originate on the NS line. Those periodicity regions are related to a pair of k-cycles born via saddle-node bifurcations (typical for smooth maps). Consider, for example, the case of the 3-cycle associated with the periodicity region colored in red. The curve SN_3 in Figure 2 indicates the occurrence of the saddle-node bifurcation in the course of which a saddle 3-cycle is born together with the attracting 3-cycle C_3. Eventually, this 3-cycle undergoes a Neimark-Sacker bifurcation at a point belonging to the curve NS_3. Note also, that the red periodicity region has a positive intersection with both the white and the light blue area. Thus, over and above the coexistence between a closed invariant curve and a 3-cycle, we might find 3-cycles to coexist with stable fixed points. Moreover, the line segment $\{(D_{12}, D_{21}) \mid D_{12} > 0.00219 \wedge D_{21} = 0.0075\}$ is intersecting a light-green area indicative of another - unrelated - fixed point. Given the scope of the paper, we will not discuss this case in the remainder.

Note that, in the course of our numerical experiments, we observed that for $p \in \Pi_k$ all sample trajectories were attracted to the respective k-cycle. In fact, close to the Neimark-Sacker bifurcation a saddle-node connection formed by the stable invariant set of the saddle k-cycle exists, and on the curve the trajectories converge to the related attracting cycle.

There exist points p such that $p \in \Pi_k$ and $p \in \Pi_l$, $k \neq l$, inside the white partition. Apparently, the respective periodicity regions are associated with different bifurcation events. As a consequence, one should be able to establish incidences of *observable co-existence* between stable k-cycles and l-cycles over and above those focused on in the sequel.

3.2. **Characterization of coexisting attractors.** This largely descriptive section reveals details about the coexisting attractors on the basis of 1D bifurcation diagrams exhibited in Figure 3.

The black solid line in Figure 2 through $D_{21} = 0.0075$ signifies the interval in the parameter plane on which we will concentrate our investigation of transitions between coexisting attractors. Fixing the influence of person 1 on individual 2 at 0.0075, we allow the influence of person 2 on individual 1 to vary over a fine grid of parameter values between 0 and 0.00245. At each grid point, a sample series $\{x\}_{t=0}^{T}$ with adequately chosen $(x_{1,0}, x_{2,0})$, is generated. To remove transient effects, only the last observations $\{x\}_{t=T-\tau}^{T}$ with $T = 2000$ and $\tau = 200$ are plotted against the respective parameter value. The resulting 1D-bifurcation plot should identify

[1] For conceptual details and/or examples see for instance [4] and [21] respectively.

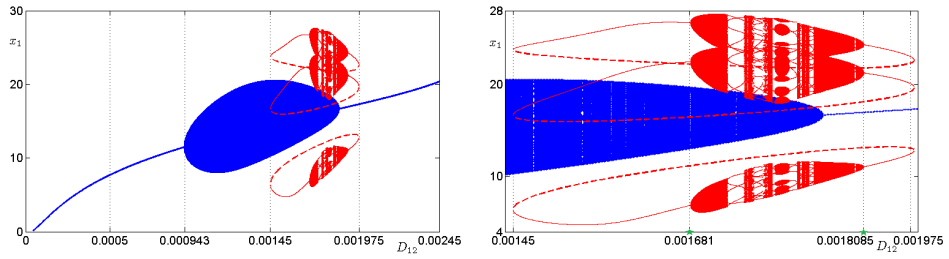

(a) (b)

FIGURE 3. For $D_{21} = 0.0075$, we give bifurcation diagrams for $0 \leq D_{12} \leq 0.00245$ linked to the horizontal black line in Figure 2 (a) and an enlargement (b) focussing on the interval $0.00145 \leq D_{12} \leq 0.001975$ over which two attractors coexists.

attractors of the underlying system. By following this approach we generated two attractor images and combined the objects in Figure 3. The figure suggests that

$$D^{ms} = \{(D_{12}, D_{21}) \mid 0.00145 \leq D_{12} \leq 0.001975 \wedge D_{21} = 0.0075\} \tag{6}$$

defines the interval of values for which *bi-stability* prevails.

Seen from an economic perspective, two types of alternative long-run consumption behavior exist. For example, there exists a window of D_{12} values such that the long-run consumption behavior is described by motion on a closed invariant curve Γ or alternatively by a 3-cycle C_3. For increased D_{12}, one type of long-run behavior is described by a closed invariant curve Γ and the alternative by a closed invariant curve consisting of three pieces Γ_3. For D_{12} values close to 0.001975, a long-run steady state consumption E coexists with a C_3. Which of the two long-run behaviors will be observed in each case depends on which basin of attraction an individuals' initial endowment (x_{10}, x_{20}) is lying. Thus, in the area of the parameter space denoted as D^{ms}, the system clearly exhibits path dependence. Having accounted for the various types of coexisting attractors, we will characterize the blue and the red attractors in detail.

The main point here is that for every level of influence $D_{12} \in (0.00145, 0.001975)$ the long-run behavior adopted by the consumers depends on where the consumption process started: in the basin of the blue attractor or in the basin of the red attractor. For the *deterministic skeleton*, we can identify several cases of coexisting long-run behavior (Γ, C_3), (Γ, Γ_3), (E, Γ_3) and (E, C_3) on the basis of Figure 3 alone. We decided to single out those cases because the coexistence prevails over relatively wide parameter windows. Thus, the chosen coexisting attractors represent robust, observable, long-run consumption behavior.

4. **Stochastic dynamics.** We will now turn to the analysis of the stochastic consumption system (1) with $\varepsilon > 0$. Our exploration focusses on the line D^{ms} in the parameter space for which *multi-stability* has been established in the subsection 3.2. In response to small perturbations, we expect the resulting random consumption trajectories to leave the deterministic attractor(s) and be randomly distributed around it (them), i.e. spend most of the time in a neighborhood of some attractor ([13]).

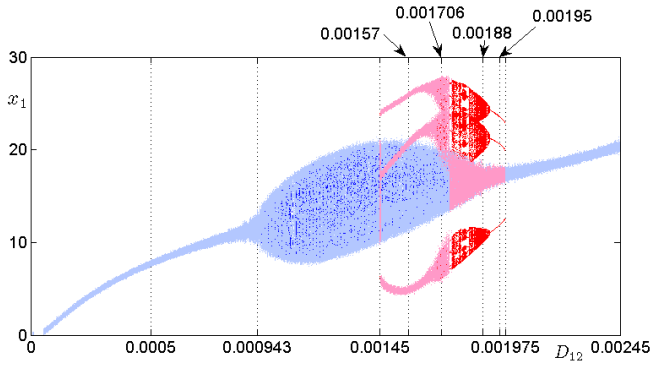

FIGURE 4. Bifurcation diagram for the case of *additive noise* with $\varepsilon = 0.1$ ($D_{21} = 0.0075$). If the initial value $(x_{1,0}, x_{2,0})$ lies on the deterministic blue (red) attractor, then elements of the trajectory are colored light blue (red).

In this first approach to the stochastic case, we report outcomes of numerical experiments involving two types of noise. The experimental results are presented in the form of 1D-bifurcation diagrams paralleling the descriptive analysis for the deterministic case. The experiments show how the random trajectories are distributed around the respective deterministic attractors, and they give a first indication for noise-induced transitions between attractors. In the subsequent step of the analysis, we study the sensitivity of attractors to various types of noise using the stochastic sensitivity function approach. Spin-offs from this analysis constitute the conceptual framework we use to study transitions occurring between various types of long-run consumption behavior.

The outcome of the first experiment involving *additive noise* is illustrated by means of the 1D bifurcation diagram shown in Figure 4. The graph was constructed as follows: Setting $\tau = 200$ and $T = 10200$ (transient time 10000) generate the 1D-bifurcation diagram for the additive noise case. The sample trajectories for which the initial value $(x_{1,0}, x_{2,0})$ lies on the blue attractor are colored light blue, while the realizations of the process started on the red attractor will be colored in light red and superimpose it on the 1D-diagram associated with the deterministic skeleton given in Figure 3. In this way we obtain information about the domain of the (marginal) invariant density of the stochastic consumption states (additive case) for a given D_{12}. Moreover, we can relate this domain to the respective deterministic attractor.

As expected, for a large non-connected range of the values of D_{12}, the light colored trajectories stay in the neighborhood of the deterministic attractor. The overlay indeed covers the deterministic attractors. The situation is clearly different for $\{(D_{12}, D_{21}) \mid 0.001748 \leq D_{12} \leq 0.001975 \wedge D_{21} = 0.0075)\}$. For this interval of D_{12} values, the stochastic trajectory tracks the deterministic blue attractor closely. After a transient phase, the light red trajectories started on the red attractor, seem to have settled in the neighborhood of the blue attractor. Thus, the outcome of the experiment indicates that transitions from the Γ_3 to the blue attractor (Γ or E or cycles) are a likely event. Note that there exists a small right neighborhood of

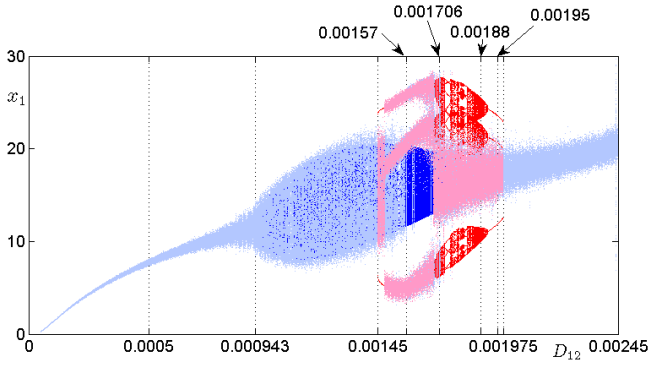

FIGURE 5. Bifurcation diagram for the case of *parametric noise* with $\varepsilon = 0.1$ ($D_{21} = 0.0075$). If $(x_{1,0}, x_{2,0})$ lies on the deterministic blue (red) attractor, then elements of the trajectory are colored light blue (red).

the bifurcation point such that for $D_{12} \in (0.00145, 0.00145 + \delta^{additive})$ the light red trajectories started on the stable 3-cycle converges to Γ. [2]

At the given noise intensity of $\varepsilon = 0.1$, the individuals' stochastic consumption trajectories will stay close to the respective deterministic blue and red attractors for $D_{12} < 0.001748$. In a sense, the behavior in the case of weak additive noise, will resemble the long-run behavior of the deterministic case. If the influence of consumer 2 on 1 exceeds this threshold, then the consumers whose initial endowment with commodities was such that their long-run behavior is described by a motion on Γ_3 or C_3 eventually change their behavior. From a certain t on, their long-run demand for x is distributed on Γ or settles on a stochastic fixed point. These types of transitions, are going to be dissected below.

Next, we turn to the experiment involving *parametric noise*. Its outcome for $\varepsilon = 0.1$ is shown in Figure 5. The diagram was constructed according to the principles underlying the construction of Figure 4 in the additive-noise context. Since the scales of the axes are identical across plots, a direct comparison of the attractors under the alternative stochastic specification is supported. Thus, we will discuss the outcome of the parametric noise scenario in comparison to the additive case.

For $D_{12} > 0.0005$ the spread of the consumption levels tends to be larger in the parametric case than in the additive case. In this area of the parameter space, parametric noise implies the higher long-run consumption volatility. Transitions from Γ (or higher order cycles) to C_3 or Γ_3 occur for values of $D_{12} \in (0.00157, 0.001706)$. This type of transition did not occur in the additive case at the noise intensity of $\varepsilon = 0.1$.

As in the additive case, transitions from Γ_3 or C_3 to blue attractor are likely to occur, yet the window of D_{12} values for which these transitions are likely events

[2]This observation can be explained as follows: We consider an interval of points, which is close to the fold bifurcation giving rise to a pair of 3 cycles. The basin of attraction of the attracting 3-cycle is bounded by the stable set of the associated saddle 3-cycle. Close to the bifurcation point, the basin of attraction might be very small. Thus, even for weak perturbations the escapes from the basin are likely.

is wider in the parametric case than in the additive case. Finally, for D_{12} in the right-neighborhood of the bifurcation point $(0.00145, 0.00145+\delta^{param})$ the light red trajectories converge to the blue attractor (see footnote 8). A comparison of the respective graphs suggests that $\delta^{param} > \delta^{additive}$, i.e. the phenomenon occurs for a wider window of influence levels D_{12} under parametric noise.

Thus, the evidence exhibited in Figures 4 and 5 supports the hypothesis that - at the noise intensity of $\varepsilon = 0.1$ - various types of transitions occur between coexisting attractors. In the context of the economic model, the essence of the numerical experiments is that even for weak shocks, we observe noise-induced transitions between long-run consumption behaviors. These changes in long-run behavior typically imply changes in the volatility of consumption.

To summarize, in the cases considered above, transitions between the respective co-existing attractors are idiosyncratic to the stochastic setting irrespective of the type of noise considered. Under the economic perspective, we thus can expect to observe transitions between long-run consumption behaviors. In the sequel, we clarify how such transitions occur using concepts related to deterministic dynamic systems and spin-offs from sensitivity analysis. In particular, we reveal conditions under which transitions between consumption behaviors become likely events.

5. **Sensitivity analysis and transition.**

A framework facilitating the analysis of transitions between coexisting attractors is introduced. The coarse descriptive analysis of Sections 3 and 4 suggests that the *morphology* of an attractor changes in response to weak noise. If the noise intensity increases it may possibly exceed the basin of attraction of the deterministic attractor. In studying the causes and consequences of such a scenario, one should benefit from a methodology suited to analyze the effect of noise on the attractors of dynamic systems.

5.1. **Sensitivity analysis for attractors.**

In the sequel, we rely on a semi-analytical approach to sensitivity analysis due to [14]. To convey the concept, we provide a sketch of the approach in the context of our model and refer the reader to the relevant literature for details. As substantiated in Section 3 the deterministic consumption system (1) possesses regular attractors. We focus on one of them, say γ, for the purpose of exposition. Let x_t denote a solution of the deterministic system (1) ($\varepsilon = 0$). The solution of the respective stochastic system ($\varepsilon > 0$) is represented as $X_t \equiv x_t(\varepsilon)$. If we consider $\Delta_t(\varepsilon) = x_t(\varepsilon) - \gamma$ and $z_t = \lim_{\varepsilon \to 0} \frac{\Delta_t(\varepsilon)}{\varepsilon}$, then - in the small noise limit - we can interpret $V_t = \mathbb{E}[z_t z_t^\top]$ as an estimate of the dispersion of random states around γ. The sensitivity of an attractor captures the variation of the stochastic trajectory X_t around the (exponentially stable) attractor.

Over two subintervals of D^{ms} there exists the stable steady state E of the deterministic skeleton (cf. Figure 3) representing the least complex long-run consumption behavior. In the case of this attractor $\gamma = E$ one reflects the variation of the stochastic trajectory X_t around the stable steady state E by means of the *sensitivity matrix* W which solves $W = FWF^\top + Q$ where $F = \frac{\partial f}{\partial x}(E)$ and $Q = g(E)g(E)^\top$, where g denotes the smooth matrix function defined in (3) evaluated at the steady state E. The matrix W approximates the covariance matrix of states. A Gaussian approximation of the density of states $\psi(x, \varepsilon)$ based on the eigenvalues $\mu_1, \dots, \mu_p$ and eigenvectors of W can be given, where in the case at hand $p = 2$.

The eigenvalues are used to quantify the sensitivity of the attractor (steady state). In the sequel $\lambda = \max(\mu_1, \dots, \mu_p)$ constitutes the stochastic sensitivity function (SSF) of the respective attractor. Based on the Gaussian approximation,

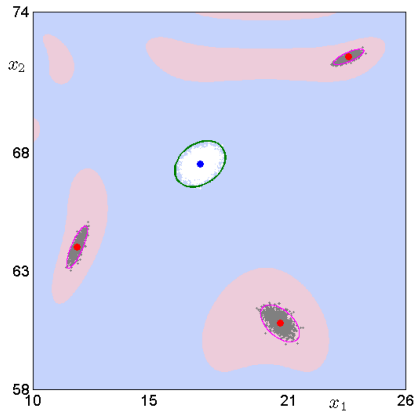

FIGURE 6. Confidence sets for fixed point E (•) and 3-cycle C_3 (•) at $D_{12} = 0.00195$, $D_{21} = 0.0075$ with trajectories superimposed ($\varepsilon = 0.1$ (white), $\varepsilon = 0.05$ (grey))

one can deduce a *confidence set* $\mathcal{C}(E, \varepsilon, \pi)$ around the attractor in which, for a given level of the noise intensity ε, the stochastic trajectory will stay with a given probability π. [3] For details see [2, p.455]. In the case at hand, such a *confidence set* takes the form of an ellipse with center E where the principle axis are related to the eigenvalues of W. For example, the magenta colored level curve superimposed on the state space in Figure 6 represents $\mathcal{C}(E, \varepsilon = 0.3, \pi = 0.99)$,[4] the confidence ellipse around the steady state E.

To obtain sensitivity functions for the coexisting attractors identified in the previous sections one proceeds in an analogous way. We provide a sketch of the procedure for a closed invariant curve. Such a curve - like Γ - is constituted by infinitely many points. The points lie dense on the attractor. One can quantify the sensitivity of the closed invariant curve to noise by considering the *sensitivity at each point* of the curve. For that purpose, one determines a hyperplane orthogonal to the closed invariant curve at a point on the curve. Next, projections of points in the neighborhood of the attractor onto the hyperplane are considered. The spread of those projections quantifies the sensitivity at the given point. It is captured by a sensitivity matrix. The eigenvalues of the sensitivity matrix summarize information about the spread. To obtain the sensitivity function for the attractor, one carries out the exercise for *many* points on the closed invariant curve. Each such point on the curve is identified by an angle ϕ relative to some pole (here "center" of the curve). The scope of this paper does not allow for an in-depth discussion of the procedure or its application to Γ_3. The intricate technical challenges are discussed,

[3] Since it is based on an approximation, the confidence set itself will not be exact. While coverage probabilities are typically excellent for simple attractors, they tend to decay for more complex attractors. An example for this phenomenon is visualized in Figure 10 (Section 7) where the confidence $\mathcal{C}(\Gamma_3, \varepsilon = 0.2)$ has a positive intersection with the immediate basin of the closed invariant curve Γ.

[4] Since we use the probability level of $\pi = 0.99$ throughout this paper, the parameter π will be dropped from the list of arguments in the sequel.

and algorithms facilitating the calculation of the sensitivity of such attractors are given in [1] and [2].

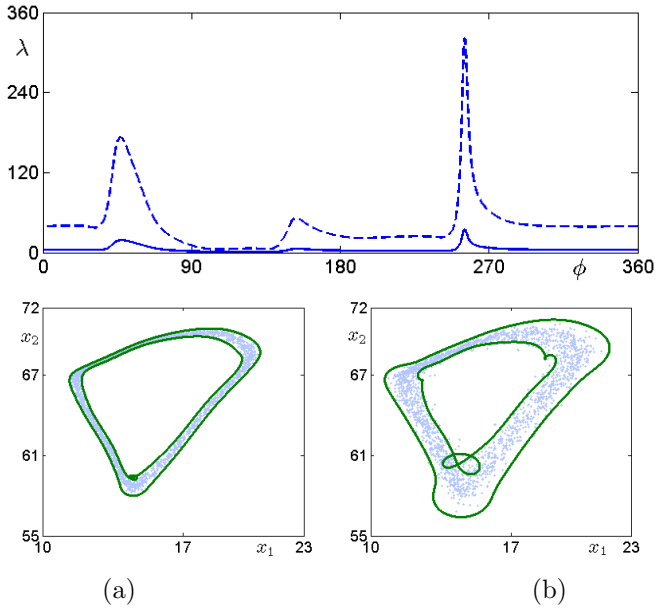

FIGURE 7. The top panel shows the graph of the sensitivity function for Γ, i.e. a plot of the maximum eigenvalue (λ) of the sensitivity matrix at a point on Γ *versus* the angle ϕ identifying the point on the attractor. The subfigures on the bottom give the confidence sets $\mathcal{C}(\Gamma, \varepsilon = 0.1)$ at $D_{12} = 0.00157$ for additive (a) and parametric noise (b).

Following this cursory introduction into sensitivity analysis, we will now illustrate the approach by showing the outcome of the sensitivity analyses for two attractors: Γ and C_3. The results for the invariant curve Γ for additive and parametric noise are shown in Figure 7. The graphs of the sensitivity functions for additive (solid line) and parametric noise (broken line) are shown in the upper panel. Apparently, the sensitivity of Γ is higher in the case of parametric noise - the case in which individual 1 is uncertain about the income of individual 2. The fact, that the dispersion around Γ is higher in the latter case, is reflected in the wider confidence band $\mathcal{C}(\Gamma, \varepsilon)$ in subfigure 7b. The pronounced peaks in the graph of the SSF suggest that the spread of the consumption trajectory around Γ varies considerably along the closed invariant curve.

The same phenomenon is visible in the following example involving Γ_3 at $D_{12} = 0.0017$. The SSF along with the confidence bands are exhibited in Figure 8. The sensitivity varies along each piece of Γ_3 and comparing the SSF's for the different pieces, we find that the spread around the red piece is considerably higher for most segments of the curve than for the other two pieces. Again, these differences in sensitivity are mirrored in the varying width of the confidence bands shown in subfigures 8c and 8d. In the remainder of this section, we will argue that sensitivity

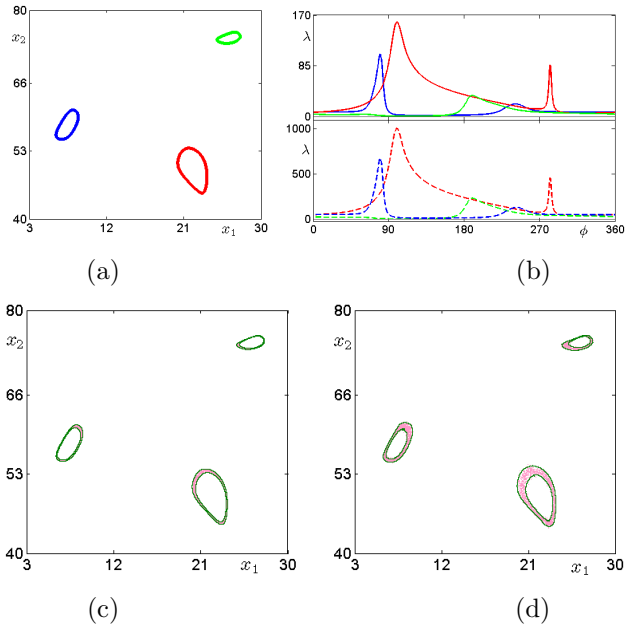

FIGURE 8. The figure shows the attractor Γ_3 at $D_{12} = 0.0017$ (a), the sensitivity functions for Γ_3 (b) as well as the related confidence sets $\mathcal{C}(\Gamma_3, \varepsilon = 0.1)$ for additive (c) and parametric noise (d).

analysis of attractors and its spin-offs can facilitate the study of transition between attractors that coexists under the deterministic skeleton.

5.2. **Transition between attractors and sensitivity analysis.** The descriptive analysis outlined in Section 3 revealed that over the subset D^{ms} of the parameter space deterministic multistability prevails as a robust, i.e. empirically relevant phenomenon. Attractors of varying complexity coexist over relatively wide parameter windows. The smooth boundaries of the basins of attraction for the respective attractors can be approximated. In addition, the confidence sets of the respective attractors can be approximated for given noise intensities in the stochastic setting.

As a result of noise, a trajectory that was started on a given deterministic attractor and stayed close to the attractor for some time, may be driven over the boundary of the attractor's basin that would have been impenetrable in the deterministic setting. In the sequel, we will refer to such an event as an *escape*. Thus, escapes occur as "large outbursts" of noise ([7, Chapter 4]) drive the process across a basin boundary. Such *noise-induced escapes* [5] are indicative of *transitions* occurring between pre-determined deterministic - possibly complex - attractors. Therefore, one has to expect that changes in the intensity of noise ε ("large outbursts" might occur more often as the intensity of noise increases) triggers qualitative changes in the evolution of the system.

Therefore, attractors which are stable under the deterministic skeleton may become *metastable* under the effect of noise. Attractors for which escape events are

[5]The phenomenon of noise-induced escape plays an important role in, for instance, models of chemical reactions or in work concerning superconducting devices (Josephson tunnel junction).

highly likely already at relatively low noise intensities are referred to as "shallow" metastable attractors ([19]). [6] An analysis of transitions occurring between two attractors would benefit from a concept measuring the "shallowness" of the attractors involved. A candidate for such a measure is the *critical intensity* defined as the smallest noise intensity ε^* for which the confidence set of a metastable attractor coincides with the boundary of the attractor's basin of attraction.

Definition 5.1. Let $\partial\mathcal{B}(\gamma)$ denote the boundary of $\mathcal{B}(\gamma)$, the basin of attraction of the deterministic attractor γ. The confidence set of the attractor at noise intensity $\varepsilon > 0$ is represented as $\mathcal{C}(\gamma, \varepsilon, \pi)$. Then, for a given confidence level π, we refer to $\varepsilon^*_\gamma = \inf\{\varepsilon \mid \mathcal{C}(\gamma, \varepsilon, \pi) \cap \partial\mathcal{B}(\gamma) \neq \emptyset\}$ as the critical noise intensity of the attractor γ.

As pointed out in Section 5.1, the confidence set $\mathcal{C}$ is based on an approximation and typically one has rely on a (numerical) approximation of the boundary $\partial\mathcal{B}$, $\varepsilon^*_\bullet$ is an approximation (or an estimate) of a true but unknown critical intensity of a given attractor.

Since the area of the confidence set of an attractor is an increasing function of ε, escapes - and therefore transitions - will become likely events for $\varepsilon > \varepsilon^*$. For noise intensities smaller than the critical intensity the trajectories can be expected to stay in a close neighborhood of the meta-attractor, rendering escapes (transitions) unlikely. Since, in the case at hand, neither the basin boundaries nor the confidence sets have an analytical representation, the critical intensities have to be obtained numerically. Attractors with low critical intensities are referred to as "shallow".

Thus, in the presence of noise, we need to clarify the relationship between the coexisting attractors. So we need to enhance the coexistence notation (γ, δ) introduced in Section 3 to capture the dynamic relationship prevailing between the attractors at a *given noise intensity* ε. To indicate that transitions between the coexisting metastable attractors γ and δ are unlikely, we use the notation $(\gamma \mid \delta)$. Should transitions be likely, arrows indicate the direction of the probable transition(s) to distinguish between $(\gamma \to \delta)$, $(\gamma \leftarrow \delta)$, and $(\gamma \rightleftarrows \delta)$.

Suppose that in the *deterministic* setting the features of the coexisting attractors γ and δ depend on a bifurcation parameter θ. In the stochastic setting, we have the additional bifurcation parameter ε. Changes in the value of the noise intensity may lead to abrupt changes in the nature of and/or relationship between the attractors in the pair (γ, δ). In the definition given below we identify the conditions in terms of (ε, θ) and the critical intensities under which the logically possible transition scenarios prevail.

Definition 5.2. Consider the bifurcation parameter θ such that (γ, δ), $\varepsilon > 0$ and $\varepsilon^*_\bullet$ as in Definition 5.1. Then

$$\varepsilon < \inf\left(\varepsilon^*_\gamma(\theta), \varepsilon^*_\delta(\theta)\right) \Rightarrow (\gamma \mid \delta) \tag{7}$$

$$\varepsilon > \sup\left(\varepsilon^*_\gamma(\theta), \varepsilon^*_\delta(\theta)\right) \Rightarrow (\gamma \leftrightarrows \delta) \tag{8}$$

$$\varepsilon^*_\gamma(\theta) > \varepsilon > \varepsilon^*_\delta(\theta) \Rightarrow (\gamma \leftarrow \delta) \tag{9}$$

$$\varepsilon^*_\gamma(\theta) < \varepsilon < \varepsilon^*_\delta(\theta) \Rightarrow (\gamma \to \delta). \tag{10}$$

The conditions under which the transition scenarios occur involve (i) global structures existing in state space for the deterministic skeleton (attractors, saddle cycle, basins, basin boundaries) and (ii) information about the likely location of states

[6] The lifetime of metastable states can be determined analytically, especially in the weak-noise limit.

under stochastic dynamics - areas of the state space traversed by the stochastic trajectory - i.e. confidence regions. Those are deduced on the basis of an approximation to the stationary density of states $\psi(\bullet, \varepsilon)$ which in turn rely on the concept of the stochastic sensitivity function.

Definition 5.2 provides the framework under which we discuss noise-induced transitions of long-run consumption behavior in the context of model (1) over the interval D^{ms} for which the coexistence of attractors has been established in subsection 3.2. Our first approach emphasizes critical intensities (Section 6), while the second approach (Section 7) features the state space perspective.

6. **Critical intensities for coexisting attractors.** The estimated critical intensities of attractors coexisting for values of the influence parameter $D_{12} \in D^{ms}$ are presented in Figure 9c. To facilitate the discussion/interpretation of those results, relevant portions of the 1D-bifurcation diagrams shown in Figures 4 and 5 have been included in Figure 9. For $D_{12} \in (0.00145, 0.00173)$ and $D_{12} \in (0.001855, 0.001974)$ the estimated critical intensities are given for the respective coexisting attractors in the cases of additive (solid lines) and parametric (broken lines) noise. For values of the bifurcation parameter $D_{12} \in (0.00173, 0.001855)$ only the critical intensities for Γ have been plotted against D_{12}. As can be inferred from Figures 9a and 9b (or Figure 3), the closed invariant curve coexists with cycles and attractors of a more complex form mostly over very narrow parameter windows, the resulting plot would hardly be informative. [7] Therefore, we do not attempt to give a complete picture over the said parameter window.

Contrasting the critical intensities of each attractor under additive and parametric noise across all segments of 9c, we conclude (i) that the critical intensity of all attractors, i.e. behaviors, considered depends on the influence parameter D_{12} and (ii) that all attractors (long-run consumption behaviors) considered so far, are more robust in the case of additive noise than in the case of parametric noise (asymmetric income uncertainty).

Next, we scrutinize/interpret the evidence given in Figure 9c adopting a different comparative angle. We contrast the critical intensities for attractors coexisting in a given parameter window and thereby demonstrate how critical intensities can be exploited for the prediction of transition events between attractors. In particular, we apply the framework for analyzing transitions outlined in subsection 5.2 to pairs of coexisting attractors found in the segments marked by 1 and 2: (Γ, C_3) and (Γ, Γ_3). The analysis of the cases in segments 4 and 5 largely parallels the previous one. It is, therefore, omitted.

(Γ, C_3): $D_{12} \in (0.00145, 0.001681)$

We have established that there exist parameter values $D_{12} \in (0.00145, 0.001681)$ such that a closed invariant curve Γ coexists with a three cycle C_3. At a given value of D_{12} a comparison of the critical intensities $\varepsilon^*_{\Gamma}(D_{12})$ and $\varepsilon^*_{C_3}(D_{12})$ allows us to assess whether transitions between attractors will occur and what type of transitions one can expect at a given noise intensity ε.

Definition 5.2 gives a condition under which transitions between metastable attractors are unlikely. Adapting (7) to our case it states that if

$$\varepsilon < min\left(\varepsilon^*_{\Gamma}(D_{12}), \varepsilon^*_{C_3}(D_{12})\right), \tag{11}$$

[7] The periods of these cycles are constrained to multiples of 3, since they are associated with the Neimark-Sacker bifurcation of C_3.

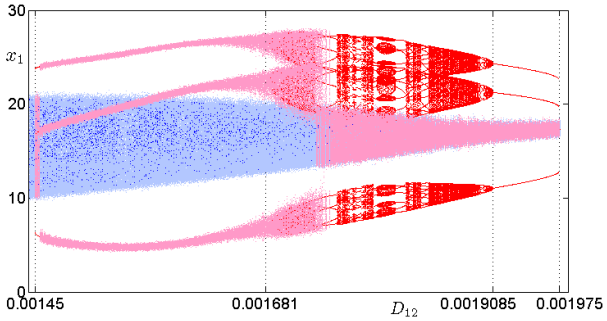

(A) Additive noise, $\varepsilon = 0.1$

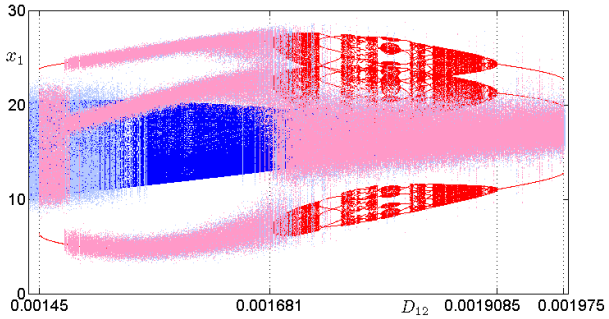

(B) Parametric noise, $\varepsilon = 0.1$

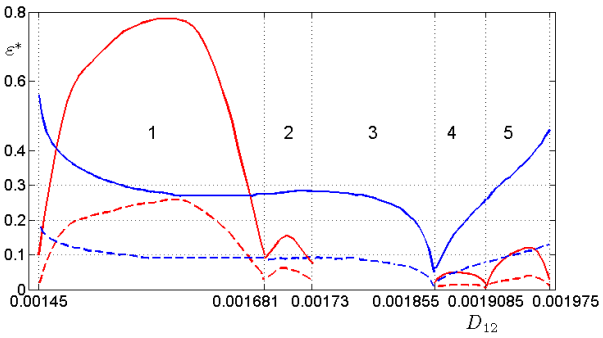

(C) Critical intensities

FIGURE 9. 1D bifurcation diagrams ((a),(b)) and critical intensities for coexisting attractors (c) with additive (solid lines) and parametric (dashed lines) noise for $D_{12} \in D^{ms}$

then transitions between the two metastable attractors are unlikely.

In our numerical experiments the noise intensity equals $\varepsilon = 0.1$ which - according to the evidence shown in Figure 9c - fulfills the inequality given above for $D_{12} \in (0.00145 + \delta, 0.001681 - \delta)$ in the case of *additive noise*. This explains the absence of transitions between the closed invariant curve and the three cycle over this interval in Figure 9a. The situation is different in the case of *parametric noise*. The evidence in Figure 9b suggests that there exists a window of D_{12} values for which

the trajectories eventually leave the basin of the Γ to stay close to the C_3. This could have been predicted since $\varepsilon = 0.1$ violates inequality (11) for $D_{12} > 0.00157$.

On the other hand, for severe levels of noise, i.e.

$$\varepsilon > max\left(\varepsilon^*_{\Gamma}(D_{12}), \varepsilon^*_{C_3}(D_{12})\right) \tag{12}$$

escapes from both respective basins might occur. The scenario $\Gamma \rightleftarrows C_3$ becomes likely, i.e. transitions in both directions will be observed.

For a wide subset of the parameter window $D_{12} \in (0.00145, 0.001681)$ we can identify noise levels that fulfill the inequality

$$\varepsilon^*_{\Gamma}(D_{12}) < \varepsilon < \varepsilon^*_{C_3}(D_{12}). \tag{13}$$

If condition (13) holds, then Γ represents shallow consumption behavior, while C_3 can be classified as a metastable consumption behavior. Therefore, the 3-cycle is a robust phenomenon over a window of D_{12} values and for a range of noise intensities. When escapes from Γ occur, the trajectory moves into the basin of the C_3. This transition is irreversible - after the escape the consumers' behavior will be described by a motion close to C_3. Therefore, condition (13) implies the case $\Gamma \rightarrow C_3$. Such a scenario has neither been documented in Figure 4 nor in Figure 5 since the noise intensity chosen for the numerical experiments ($\varepsilon = 0.1$) is simply too small to satisfy condition (13).

In the case at hand, irrespective of the type of noise, we find that the C_3 is the more robust phenomenon. The noise levels needed to induce the trajectories to escape $\mathcal{B}(C_3)$ are clearly higher than those necessary to trigger transitions from Γ to the cycle. Thus, C_3 represents consumption behavior that is *sustainable* even under considerable environmental shocks.

In Figure 9c, close to the end points of the parameter window for which C_3 exists - close to the bifurcation points - we find levels of ε such

$$\varepsilon^*_{\Gamma}(D_{12}) > \varepsilon > \varepsilon^*_{C_3}(D_{12}). \tag{14}$$

According to Definition 5.2, for such noise intensities, the transition event $\Gamma \leftarrow C_3$ becomes likely. A trajectory that starts on Γ will stay close to the attractor, while consumption trajectories starting on the C_3 will escape $\mathcal{B}(C_3)$ and converge to Γ. For the noise intensity of $\varepsilon = 0.1$ used in our numerical experiment, inequality (14) holds for a range of D_{12} values. A window for which outcomes $\Gamma \leftarrow C_3$ materialize has been identified in Figures 9a and 9b.

(Γ, Γ_3): $D_{12} \in (0.001681, 0.00173)$

For each value of the influence parameter in this window, we find $\varepsilon^*_{\Gamma}(D_{12}) > \varepsilon^*_{\Gamma_3}(D_{12})$ in the additive as well as in the parametric case. Consequently, we have to distinguish only between 3 cases irrespective of the nature of the noise: (i) If $\varepsilon < \varepsilon^*_{\Gamma_3}(D_{12})$ then $(\Gamma|\Gamma_3)$; (ii) if $\varepsilon^*_{\Gamma_3}(D_{12}) < \varepsilon < \varepsilon^*_{\Gamma}(D_{12})$ then $\Gamma \leftarrow \Gamma_3$; (iii) if $\varepsilon > \varepsilon^*_{\Gamma}(D_{12})$ then $\Gamma \rightleftarrows \Gamma_3$.

In case (i) both attractors represent metastable long-run consumption behaviors. The system is characterized by path dependence. This case is illustrated in Figure 9a which reflects the *additive noise* case for a noise intensity of 0.1. Over the parameter window scrutinized, trajectories started on Γ_3 stay close to the deterministic attractor (3 light red pieces) while the consumption process closely tracks Γ, if its initial value lies on this deterministic attractor.

Case (ii) the 3-piece closed invariant curve represents a shallow state and, in all likelihood, the direction of the transition from $\Gamma \leftarrow \Gamma_3$ will not be reversed. Turning

to the *parametric noise* scenario captured in Figure 9b, we see that for $D_{12} \in (0.001681, 0.00173)$ we are dealing with case (ii): the 3-piece closed invariant curve represents a shallow state and, in all likelihood, the direction of the transition from $\Gamma \leftarrow \Gamma_3$ will not be reversed. The noise intensity of 0.1 exceeds $\varepsilon^*_{\Gamma_3}(D_{12})$ (cf. the broken red line in Figure 9c). Escapes from the basin of the three piece closed invariant curve Γ_3 tend to materialize. Once a transition event $\Gamma \leftarrow \Gamma_3$ has occurred, the realizations of the consumption process are distributed over a neighborhood around the Γ – indicated by the light red overlay covering the Γ. Since $\varepsilon = 0.1$ almost coincides with the critical intensity $\varepsilon^*_{\Gamma}(D_{12})$, trajectories originating on the deterministic attractor Γ will - most likely - stay close to it.

Under case (iii), both long-run consumption behaviors are classified as metastable. Transitions in both directions occur. We cannot demonstrate case (iii), since the noise intensity chosen for the numerical experiment is too low. The case of the coexisting (Γ, Γ_3) will be reexamined under a state space perspective in Section 7 (cf. Figure 10). The intervals of ε values shown in Figure 9c leading to the different dynamics are based on estimates of critical intensities. It might, therefore, further our understanding of escaping trajectories (transitions) to show confidence sets and immediate basins of attraction together. Thus, we adopt a *state space perspective* in the next section.

7. **A state space perspective of transitions.**

For the case of additive noise, we reveal details of the conditions under which escapes come about and demonstrate features of the transitions occurring at various levels of the bifurcation parameter ε. The scenario analyzed involves two types of closed invariant curves , i.e. (Γ, Γ_3) at $D_{12} = 0.001706$ portrayed in Figure 10. After discussing a baseline situation, we consider a sequence of increasing noise intensities and scrutinize the respective scenarios unfolding in state space.

On the basis of the 1D-bifurcation plot shown in Figure 4 one would conjecture that at the noise intensity of $\varepsilon = 0.1$ the coexisting attractors (Γ, Γ_3) represent metastable consumption behaviors. A consumption trajectory starting on Γ will stay in its neighborhood. The same holds for trajectories originating anywhere on Γ_3. To demonstrate why transitions between the respective attractors eventually become likely under an increase of the intensity of additive noise ε, we turn to the state space representation given in Figure 10.

The state space representation shows the closed invariant curve Γ (surrounding the unstable fixed point E indicated by a blue circle coexisting with a closed invariant curve that consists of three pieces Γ_3, each of which encompasses an element of the now unstable C_3 indicated by a red circle. In addition, we find the periodic points of a saddle 3-cycle indicated by red triangles. Stable manifolds associated with the periodic points constituting this saddle cycle generate the boundaries between the immediate basins $\mathcal{B}(\Gamma_3)$ and $\mathcal{B}(\Gamma)$ while the respective unstable manifolds "connect" the attractors. [8] Thus, the saddle cycle, or better the manifolds associated with the periodic points constituting the cycle, generate a structure on the state space that facilitates the description of evolution of the deterministic process. The stochastic nature of the consumption process studied here, is reflected in the boundaries of the confidence sets for a given attractor which are superimposed on

[8]The numerical approximations of the manifolds were obtained by tools given in [15]. Points (states) on the part of the manifold lying inside the basin of an attractor are mapped onto the respective attractor along the manifold.

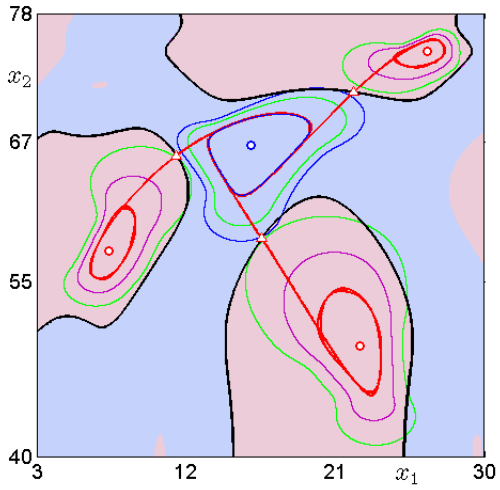

FIGURE 10. For $(D_{12}, D_{21}) = (0.001706, 0.0075)$ we show the state space representation of the coexisting attractors Γ_3 (dark red curves) and Γ (blue curve) together with their immediate basins $\mathcal{B}(\Gamma_3)$ (light red) and $\mathcal{B}(\Gamma)$ (light blue). The confidence sets are superimposed ($\varepsilon \in \{0.1, 0.2, 0.3\}$). Periodic points (red triangles) of the 3-saddle cycle are exhibited together with its stable (black lines) and unstable (red lines) manifolds. In addition, the unstable fixed point E (blue circle) and the unstable 3-cylce (periodic point given by red circles) are given.

the state space. In the case of Γ_3 such a set would consist of 3 *confidence bands*. In Figure 10, we only mark the outer boundaries – colored in magenta, green and blue – since those alone are sufficient to support our argument.

At the baseline $\varepsilon = 0.1$, we find $\mathcal{C}(\Gamma_3, 0.1) \subset \mathcal{B}(\Gamma_3)$. Since almost all consumption states will be realized inside the confidence sets (magenta colored outer boundaries) which lie at a distance from the respective basin boundaries, it is not yet likely to observe a consumption trajectory crossing the basin boundary to approach the coexisting metastable attractor Γ. This situation changes as the noise intensity is increased by 0.1.

At $\varepsilon = 0.2$, the transition event $\Gamma_3 \to \Gamma$ can be expected to materialize, since $\mathcal{C}(\Gamma_3, 0.2) \cap \mathcal{B}(\Gamma) \neq \emptyset$. The intersection is still small, i.e. the noise intensity just exceeds the respective critical intensity. At this noise level it is not unlikely to witness escapes from Γ_3 to Γ, while it is not yet probable to return to Γ_3 from the Γ. This is so, since $\mathcal{C}(\Gamma, 0.2) \subset \mathcal{B}(\Gamma)$, i.e. the confidence set of the Γ is still a true subset of the basin of Γ. This changes as the level of noise is increased to $\varepsilon = 0.3$.

Focussing on the relationship prevailing between the confidence set and the basin of attraction for the Γ, we find that $\mathcal{C}(\Gamma, 0.3) \cap \mathcal{B}(\Gamma_3) \neq \emptyset$ holds. Again, the intersection is small, since we have chosen an ε that just exceeds the critical intensity for an escape from Γ (cf. Figure 9 - height of solid blue line at $D_{12} = 0.001706$). Thus, at the level of noise considered the event $\Gamma_3 \leftrightarrows \Gamma$ might materialize. Transitions can occur in either direction. Both metastable consumption behaviors would be classified as "shallow".

Relying on sensitivity analysis we have identified and explained the conditions under which transitions between coexisting metastable attractors (long-run consumption behaviors) will be observed. As detailed in subsection 5.1 the confidence set for a given metastable attractor allows us to predict which area of the state space a consumption trajectory will traverse most of the time. But so far it remains an open question whether the prediction and/or description of a *typical transition path* can be facilitated.

To discuss this problem it is constructive to draw the reader's attention to a condition that is portrayed in Figure 10. At the critical intensity $\varepsilon^*_\bullet$, the confidence set "touches" the immediate basin at - or in the neighborhood of - one of the periodic points (Δ) of the saddle cycle. This suggests that the path taken by a consumption trajectory during an escape and transition episode may be determined in a decisive way by the saddle 3-cycle. [9]

In the related literature, our problem of describing transition behavior, is framed as the search for a most probable escape path (MPEP). For examples, see [17], [13] or [19]. For a few systems it has been possible to solve the problem analytically. [19], for instance, determine an appropriate Hamiltonian trajectory to describe the path which the noisy system is likely to follow during an escape and transition episode. The majority of the efforts aiming at the identification of the MPEP is of an experimental nature. The existing research efforts converge to the findings that (i) for weak noise, it is most likely to escape a metastable attractor, by passing through the neighborhood of a saddle point lying on the basin boundary by definition. Moreover, (ii) the trajectory typically leaves the metastable attractor along the direction of the associated saddle cycle's unstable manifold.

These findings also resonate in the experiments of [11] who analyze the transitions occurring in the case of 2-cycle coexisting with a steady state (see Figures 9, 10 in therein). To explore whether the findings outlined above also apply to the current more complex situation, we superimpose a single sample trajectory on the state space representation of the case (Γ, Γ_3) exhibited in Figure 10.

Figure 11 supports the claim that for complex attractors noise-induced transitions are determined by the unstable manifold(s) of the saddle 3-cycle. The existing findings lead to the conjecture that the most probable complex transition trajectories possesses an identifiable strong deterministic component. In the context of our stochastic consumption model (1), it is a feature of the deterministic skeleton that, in a sense, *governs* the consumption behavior in the transition phase.

8. **Discussion and conclusion.**

We analyze the dynamics of the stochastic consumption model (1) with levels of the influence parameter D_{12} and the noise intensity ε being constrained to the set $\{(\varepsilon, D_{12}) \mid \varepsilon \geq 0 \wedge D_{12} \in D^{ms}\}$ for additive as well as parametric noise. Our approach to noise-induced transition between long-run consumption behaviors rests on information concerning dynamic modes generated by the deterministic skeleton of (1). The key finding from this initial stage of the analysis points to the coexistence of attractors. In particular, as the effect of individual 2's past consumption choices on the current preferences of the first individual grows, the sequence of pairs of coexisting long-run consumption behaviors (attractors) (Γ, C_3), (Γ, Γ_3), (E, Γ_3), and (E, C_3) evolves or unfolds. Over

[9] Also notice that the major axes of confidence sets tend to be oriented in the direction of the respective elements of the saddle cycle! This may be viewed as a first hint at the relevance of the saddle cycle and its unstable manifold for the transition process.

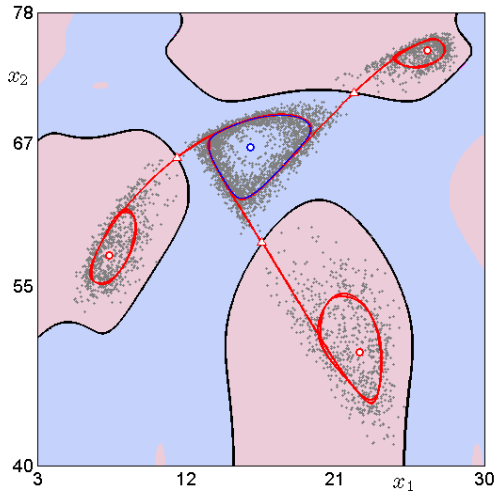

FIGURE 11. (Γ, Γ_3) at $(D_{12}, D_{21}) = (0.001706, 0.0075)$ with sample trajectory (single simulation run with $\varepsilon = 0.2$) superimposed

the parameter window considered, the complexity of the blue attractor reduces from closed invariant curve to steady state, while the complexity of the coexisting red attractor increases from 3-cycle to 3-piece closed invariant curve and then decreases again to a simple 3-cycle. Thus, the influence parameter does not only affect intricate characteristics of each attractor, but it also determines what types of long-run behaviors coexist. Over the parameter region investigated the deterministic system exhibits path dependence.

The subsequent analysis shows the consumption system looses this property eventually under increasing the noise intensities. But at sufficiently low levels of ε we can establish a sequence of coexisting metastable attractors ($\Gamma|C_3$), ($\Gamma|\,\Gamma_3$), ($E|\,\Gamma_3$), and ($E|C_3$). Under weak perturbations, the consumption process will closely track the attractor on which it was started. Apart from small neighborhoods around the bifurcation points lying in the window for D_{12} all coexisting long-run behaviors can be classified as metastable.

For low levels of the influence $0.001468 < D_{12} < 0.001666$ the coexisting long-run consumption behaviors are considerably robust. In particular, C_3 is more robust to noise than the coexisting closed invariant curve. Escapes from this attractor become likely only under significant noise levels. Under intermediate noise transitions from a relatively simple cyclical consumption behavior to more complex behavior (motion on a closed invariant curve) are probable. The direction of the transitions is reversed in the neighborhood of the bifurcation points.

The situation changes drastically for higher levels of influence. For $D_{12} > 0.0018855$ the long-run behaviors associated with Γ_3 and C_3 become "shallow". Already at low noise intensities behavioral transition become likely. For noise intensities in an intermediate range, trajectories started on any of the red attractors will converge to a stochastic steady state. These qualitative statements hold irrespective of the type of noise considered.

For the region of the parameter space studied, we can conclude that in a moderate noise environment increased peer influence actually reduces the complexity of observable long-run consumer behavior as more complex behavioral alternatives become shallow. Moreover, we present some evidence suggesting that models of transitions between complex coexisting attractors would have to rely on a strong deterministic component linked to an existing saddle cycle.

Although the region of multistability analyzed in this paper differs from the one scrutinized in [11], the results outlined above parallel the earlier findings. In particular both analyses culminate in the finding that more complex attractors become less robust phenomena as influence parameter D_{12} increases. In addition, we observe that the unstable manifold of a saddle cycle plays a crucial role for the transition dynamics. That is, our current findings support and robustify the conclusions reached by [11].

Turning to limitations of our study, we have to acknowledge that our results - when seen from a mathematical perspective - are not "generic" with respect to model (1), since our investigation focuses on a narrow interval of values for influence parameter D_{12} holding all other parameters fixed. In fact, as far as we know, a complete description of the dynamics of (1) in a generic case has not been provided. Such a description poses a challenging task for future research. Moreover, only two types of stochastic perturbations have been considered. In future efforts, a broader spectrum of - economically meaningful - noises could should be included.

In addition, we anticipate three future research efforts addressing problems that arose in the course of our analysis. First of all, we need to improve the characterization of transition processes in the neighborhood of bifurcation points. Secondly, one should address the question of whether the framework has the potential to support the development of criteria indicating that the system is about to enter a transition episode. And finally, we will attempt to provide a detailed assessment of the effect of different types of noise on the escape mechanism and the structure of the transition trajectories. The objective of providing representations of transition paths adequately capturing the distribution of states around the unstable manifolds could be pursued by following the experimental/numerical approach implemented in [17].

Acknowledgments. Tatyana Perevalova and Jochen Jungeilges gratefully acknowledge research funding from the Ministry of Science and Higher Education of the Russian Federation (Ural Mathematical Center project No. 075-02-2021-1387).

REFERENCES

[1] I. Bashkirtseva and L. Ryashko, Stochastic sensitivity of the closed invariant curves for discrete-time systems, *Phys. A*, **410** (2014), 236–243.

[2] I. Bashkirtseva, L. Ryashko and A. Sysolyatina, Analysis of stochastic effects in Kaldor-type business cycle discrete model, *Commun. Nonlinear Sci. Numer. Simul.*, **36** (2016), 446–456.

[3] J. Benhabib and R. H. Day, Rational choice and erratic behaviour, *Rev. Econom. Stud.*, **48** (1981), 459–471.

[4] H. W. Broer, M. Golubitsky and G. Vegter, Geometry of resonance tongues, *Singularity Theory*, 327–356, World Sci. Publ., Hackensack, NJ, (2007). https://www.researchgate.net/publication/252963138_Geometry_of_resonance_tongues

[5] E. Ekaterinchuk, J. Jungeilges, T. Ryazanova and I. Sushko, Dynamics of a minimal consumer network with bi-directional influence, *Commun. Nonlinear Sci. Numer. Simul.*, **58** (2018), 107–118.

[6] E. Ekaterinchuk, J. Jungeilges, T. Ryazanova and I. Sushko, Dynamics of a minimal consumer network with uni-directional influence, *Journal of Evolutionary Economics*, **27** (2017), 831–857.

[7] M. I. Freidlin and A. D. Wentzell, *Random Perturbations of Dynamical Systems*, 3rd edition, Springer, Heidelberg, 2012.
[8] W. Gaertner and J. Jungeilges, A non-linear model of interdependent consumer behaviour, *Economics Letters*, **27** (1988), 145–150.
[9] W. Gaertner and J. Jungeilges, "Spindles" and coexisting attractors in a dynamic model of interdependent consumer behavior: A note, *Journal of Economic Behavior & Organization*, **21** (1993), 223–231.
[10] J. Jungeilges, E. Maklakova and T. Perevalova, Stochastic sensitivity of bull and bear states, *Journal of Economic Interaction and Cooperation*, (2021).
[11] J. Jungeilges and T. Ryazanova, Transitions in consumption behaviors in a peer-driven stochastic consumer network, *Chaos Solitons Fractals*, **128** (2019), 144–154.
[12] J. Jungeilges, T. Ryazanova, A. Mitrofanova and I. Popova, Sensitivity analysis of consumption cycles, *Chaos*, **28** (2018), 055905, 12 pp.
[13] Z. Li, K. Guo, J. Jiang and L. Hong, Study on critical conditions and transient behavior in noise-induced bifurcations, *Control of Self-Organizing Nonlinear Systems*, 169–187, Underst. Complex Syst., Springer, [Cham], (2016).
[14] G. Mil'shtein and L. Ryashko, The first approximation in the quasipotential problem of stability of non-degenerate systems with random perturbations, *Journal of Applied Mathematics and Mechanics*, **59** (1995), 47–56.
[15] A. Panchuk, CompDTIMe: Computing one-dimensional invariant manifolds for saddle points of discrete time dynamical systems, *Gecomplexity Discussion Paper Series 11*, Action IS1104 "The EU in the new complex geography of economic systems: Models, tools and policy evaluation", 2015, https://EconPapers.repec.org/RePEc:cst:wpaper:11.
[16] L. Ryashko, Noise-induced transformations in corporate dynamics of coupled chaotic oscillators, *Mathematical Methods in the Applied Sciences*.
[17] A. N. Silchenko, S. Beri, D. G. Luchinsky and P. V. E. McClintock, Fluctuational transitions through a fractal basin boundary, *Phys. Rev. Lett.*, **91** (2003), 174104.
[18] E. Slepukhina, L. Ryashko and P. Kügler, Noise-induced early afterdepolarizations in a three-dimensional cardiac action potential model, *Chaos, Solitons & Fractals*, **131** (2020), 109515.
[19] Y. Tadokoro, H. Tanaka and M. I. Dykman, Noise-induced switching from a symmetry-protected shallow metastable state, *Scientific Reports*, **10** (2020), 1–10.
[20] J. Xu, T. Zhang and K. Song, A stochastic model of bacterial infection associated with neutrophils, *Appl. Math. Comput.*, **373** (2020), 125025, 12 pp.
[21] Z. T. Zhusubaliyev, E. Soukhoterin and E. Mosekilde, Quasiperiodicity and torus breakdown in a power electronic dc/dc converter, *Math. Comput. Simulation*, **73** (2007), 364–377.

Received November 2020; revised July 2021; early access September 2021.

E-mail address: jochen.jungeilges@uia.no
E-mail address: trygve.k.nilssen@uia.no
E-mail address: tatyana.perevalova@urfu.ru
E-mail address: aleksandr-satov@mail.ru